Acta Cryst. (1997). D53, 406–418

Structures of a Blue-Copper Nitrite Reductase and its Substrate-Bound Complex

FRASER E. DODD,[a,b] S. SAMAR HASNAIN,[a,b]* ZELDA H. L. ABRAHAM,[c] ROBERT R. EADY[c] AND BARRY E. SMITH[c]

[a]*Molecular Biophysics Group, Synchrotron Radiation Department, CCLRC Daresbury Laboratory, Warrington WA4 4AD, England,* [b]*De Montfort University, Leicester LE1 9BH, England, and* [c]*Nitrogen Fixation Laboratory, John Innes Centre, Norwich NR4 7HU, England. E-mail: s.hasnain@dl.ac.uk*

(Received 7 October 1996; accepted 10 February 1997)

Abstract

Copper-containing nitrite reductases (NiR's) have been conveniently subdivided into blue and green NiR's which are thought to be redox partners of azurins and pseudo-azurins, respectively. Crystal structures of two green NiR's have recently been determined. *Alcaligenes xylosoxidans* has been shown to have a blue-copper nitrite reductase (AxNiR) and two azurins with 67% homology both of which donate electrons to it effectively. The first crystal structure of a blue NiR (AxNiR) in its oxidized and nitrite-bound forms, with particular emphasis to the Cu sites, is presented. The Cu–Smet distance is the same as those in the green NiR's. Thus, the length of this interaction is unlikely to be responsible for differences in colour. Crystallographic data presented here taken together with structural data of other single Cu type-1 proteins and their mutants suggest that the displacement of Cu from the strong ligand plane is perhaps the cause for the differences in colour observed for otherwise 'classical' blue Cu centre. Nitrite is observed binding to the catalytic Cu in a bidentate fashion displacing the water molecule, offering a neat rationalization for the XAFS observation that the type-2 Cu–ligand distances increase on nitrite binding as a result of increased coordination. These results are discussed in terms of enzyme mechanism.

1. Introduction

Dissimilatory nitrite reductase (NiR) is a key enzyme in the anaerobic respiratory pathway of denitrifying bacteria where nitrate is sequentially reduced to the gaseous products NO, N_2O or N_2, leading to a significant loss of fixed nitrogen from the terrestrial environment (Payne, 1985). The NiR from *A. xylosoxidans* (NCIMB 11015) (AxNiR) (Abraham, Lowe & Smith, 1993) belongs to the group of NiR's which utilize copper at the redox active centres. All Cu NiR's isolated so far have a strong band near 600 nm arising from a (Cys)S $\rightarrow$ Cu^{II} charge transfer which is characteristic of a type-1 Cu centre. The ratio of intensity of this band to a second charge-transfer absorption band at ~460 nm determines whether a Cu NiR is blue or green in colour (Han *et al.*, 1993). AxNiR belongs to the subset of Cu-NiR's which are blue in colour and are thought to have azurin as the electron partner.

So far, ten copper-containing NiR's are known, four of which have been sequenced; *Achromobacter cycloclastes* (AcNiR) (Fenderson *et al.*, 1986), *Alcaligenes faecalis* S-6 (AfNiR) (Nishiyama *et al.*, 1993), *Pseudomonas sp.* G179 (Ye, Averill & Tiedje, 1992) and *Pseudomonas aureofaciens* (PaNiR) (Glocker, Jüngst & Zumft, 1993); show a high sequence identity. Two of the copper-containing enzymes have been crystallographically characterized, namely those from *A. cycloclastes* (Godden *et al.*, 1991) and *A. faecalis* S-6 (Kukimoto *et al.*, 1994). Both of these belong the subset of Cu-NiR's which are green in colour. In both cases a pseudo-azurin (not azurin) has been identified as electron donor (Kakutani, Watanabe, Arima & Beppu, 1981) and the structure of a pseudo-azurin from *A. faecalis* S-6 has been determined (Adman *et al.*, 1989). Pseudo-azurins differ from azurins in several respects but in particular they lack the disulfide bridge and the back flap, the latter aspect has been suggested to be responsible for pseudo-azurins specificity to the green NiR's (Adman *et al.*, 1989). In *A. xylosoxidans* (Ax), two distinct azurins with 67% homology to each other have been identified, both of which have been shown to be effective electron donors to the blue NiR from this organism (Dodd, Hasnain, Hunter *et al.*, 1995). There are several blue Cu-NiR's known but only the NiR from *P. aureofaciens* (PaNiR) has been sequenced (Glocker *et al.*, 1993). The two green NiR's show a higher identity among themselves than to the blue NiR, Fig. 1.

The trimeric structures of several of these NiR's have now been established by X-ray crystallography and solution scattering. Two green NiR's, AcNiR and AfNiR, have been shown to be trimers in the crystal while the latter has also been shown to be a trimer in solution also by X-ray scattering (Kukimoto *et al.*, 1994; Dodd *et al.*, 1993). Two blue NiR's, AxNiR (Grossmann *et al.*, 1993) and PaNiR (Grossmann, Hasnain & Zumft, manuscript in preparation) have also been shown to possess the trimeric structure by solution X-ray scattering. Crystal structures of both of the green NiR's, AcNiR and AfNiR, show that they are similar with the monomer consisting of two domains with Greek key β-barrels similar to those found in cupredoxins such as azurin. Each monomer

contains a type-1 Cu site buried in each of the subunits and the type-2 Cu sites located at the subunit interfaces with ligands to the Cu atom provided from adjacent monomers. This trimeric arrangement results in a total of six Cu atoms per molecule. Spectroscopic studies of the AxNiR have shown that it also contains both type-1 and type-2 copper (Abraham *et al.*, 1993). The type-2 site has been demonstrated to bind nitrite (Howes *et al.*, 1994; Strange *et al.*, 1995). The activity of AcNiR and AxNiR have been shown to correlate with the occupancy of the type-2 copper site (Libby & Averill, 1992; Abraham *et al.*, 1993). Electron nuclear double resonance spectroscopy of nitrite-bound oxidized AxNiR (Howes *et al.*, 1994) has shown that the nitrite binds to the type-2 copper *via* an O atom since no effect of isotopic substitution of ^{15}N into nitrite was observed. XAFS studies of nitrite bound AxNiR (Strange *et al.*, 1995) has shown that the nitrite binds to the type-2 copper with a Cu—O distance of 1.98 Å and that the Cu—His distances increasing, presumably causing an expansion of the type-2 Cu by ~0.08 Å upon binding of nitrite. Crystallographic studies of nitrite-soaked AcNiR (Adman, Godden & Turley, 1995) suggests that nitrite binds to the type-2 copper *via* O atoms in a bidentate fashion at a distance of ~2.2 and 2.5 Å.

2. Experimental

2.1. *Crystallization*

Single crystals of AxNiR were grown by the sitting-drop vapour-diffusion method at 277 K using 28% PEG 4000, 0.1 *M* sodium acetate and 0.2 *M* ammonium ac-

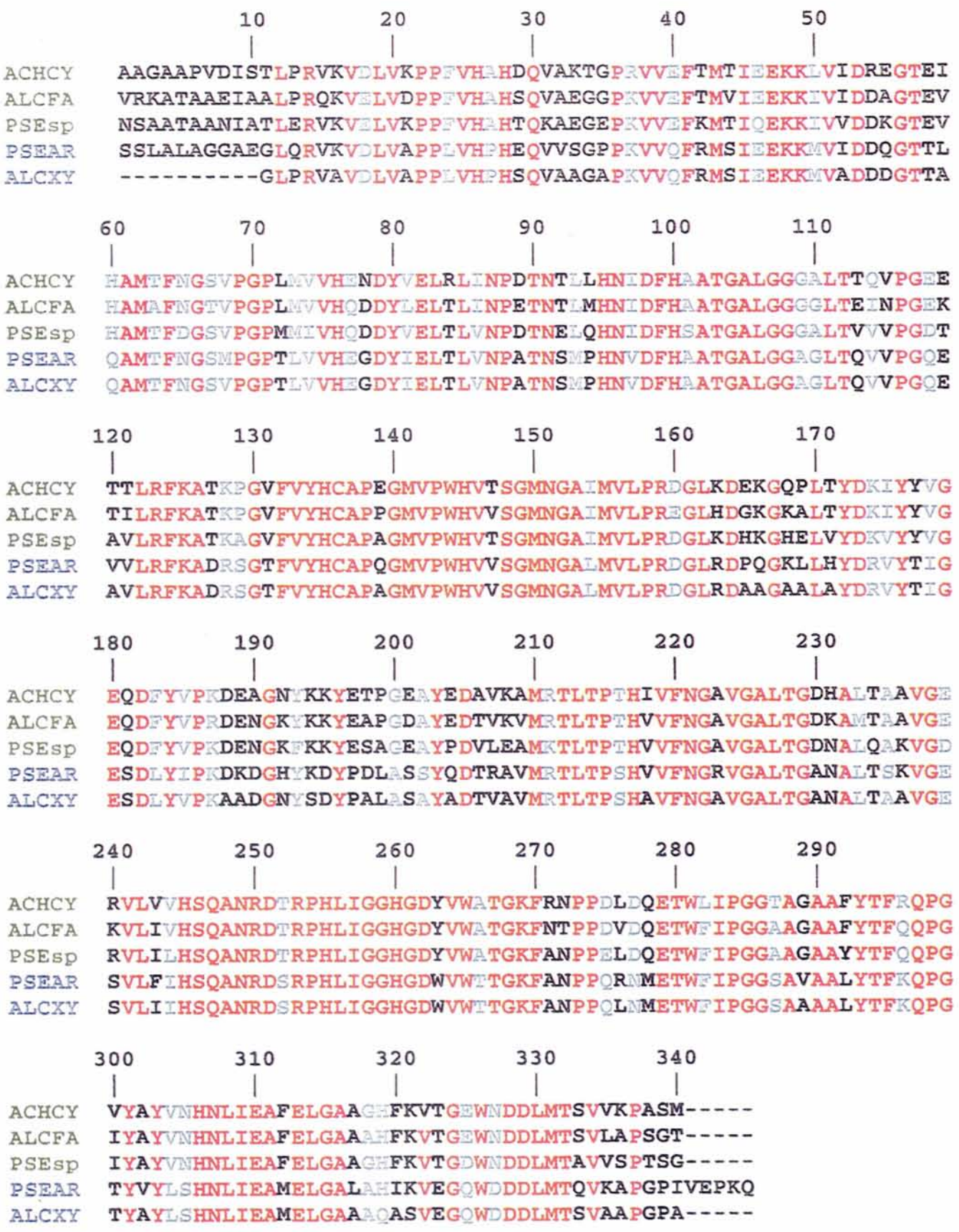

Fig. 1. Sequence alignment of the NiR's. ACHCY, *Achromobacter cycloclastes*; ALCFA, *Alcaligenes faecalis*; PSEsp, *Pseudomonas sp.* (strain G-179); PSEAR, *Pseudomonas aureofaciens*; ALCXY, sequence used in *A. xylosoxidans*. Identities are shown in red and similarities in blue. Sequence information was acquired from *SEQNET* and alignment preformed using *CLUSTALV* (Higgins, Bleasby & Fuchs, 1992).

etate at pH 4.6. The drops consisted of 3 µl reservoir and protein solutions. The AxNiR solution was at a concentration of 10 mg ml^{-1} in a 20 m*M* MES pH 6.0 buffer. Crystals appeared in around 3 weeks and grew in a few days as large plates. The crystals grew to maximal dimensions of 2.0 × 0.5 × 0.05 mm. The crystals are blue and remain unchanged in their appearance for months. The colour of the crystals is consistent with the enzyme being in the oxidized form *i.e.* Cu in Cu^{2+} state.

2.2. *Data collection*

Data for AxNiR were collected at the Photon Factory, KEK at beamline BL6A-2 using the Weissenberg technique (Sakabe 1991) with Fuji image plates (200 × 300 mm) an BA100 scanning system. The X-ray wavelength was 1.0 Å. The crystal-to-image-plate distance was 429.7 mm. A total of 90.3° of data were collected from three crystals at a temperature of 286 K. The data were integrated using *WEIS* (Higashi, 1989), then scaled and merged using *CCP*4 (Collaborative Computational Project, Number 4, 1994). Crystals belong to the space group $P2_12_12_1$ with unit-cell parameters $a = 67.2$, $b = 101.7$, $c = 150.4$ Å. The data had a merging R factor of 8.5% and a completeness of 79.3% at 3.0 Å (Table 1).

Crystals of AxNiR, which were macroseeded for the original crystals at 20% PEG 4000, were soaked such that there was a tenfold excess of nitrite (2 m*M* $NaNO_2$) to each monomer. The soaking time for the crystals was ~2 h. These crystals retained their original blue colour upon soaking. Data were collected from the nitrite-soaked crystals using the MAR image plate at station 9.5 (Thompson *et al.*, 1992) at the SRS, Daresbury, England. The data were integrated using *DENZO* (Otwinowski, 1993) and scaled and merged using *CCP*4 (Weeg-Aerssens, Tiedje & Averill, 1988). The refined unit-cell parameters were $a = 67.9$, $b = 102.2$, $c = 151.9$ Å. The data had a merging R factor of 5.3% and a completeness of 91.9% at 2.8 Å (Table 1).

2.3. *Software*

Molecular replacement was carried out using *AMoRe* (Navaza, 1994) and the maps calculated in *CCP*4. Model building was performed with *O* (Jones, Zou, Cowan & Kjeldgaard, 1991). Refinement was performed using *X-PLOR* (Brünger, 1992). Structural quality check of the model were performed with *PROCHECK* (Laskowski, MacArthur, Moss & Thornton, 1993) Additional graphical work was carried out in *O* and *INSIGHT*II. Figs. 5 and 9 were prepared using *MOLSCRIPT* (Kraulis, 1991).

2.4. *Molecular replacement*

The structure was solved by molecular replacement using *AMoRe* (Navaza, 1994) using the 2.6 Å refined structure of the NiR trimer (excluding solvent) from *A. faecalis* S-6 (AFN1, Kukimoto *et al.*, 1994). The rotation function yielded three clear solutions which were related by the threefold symmetry of the starting model. The translation function gave one outstanding solution which, after rigid-body refinement, yielded an R factor of 33.9% and a correlation coefficient of 0.68.

Table 1. *Summary of data-reduction statistics*

	AxNiR	AxNiR plus NO_2
Cell axes a, b, c (Å)	67.2, 101.7, 150.4	67.9, 102.2, 151.9
Diffraction limit (Å)	3.0	2.8
No. of observed reflections	53045	76663
No. of independent reflections	16691	24356
Highest resolution shell (Å)	3.13–3.00	2.87–2.80
Completeness (%)		
All data	79.3	91.9
Highest resolution shell	57.6	82.5
R_{sym} (on I)* (%)		
All data	8.5	5.3
Highest resolution shell	17.4	10.2
$I/\sigma(I)$		
All data	8.1	9.2
Highest resolution shell	4.2	6.2

* $R_{sym}(I) = \sum_{hkl}\sum_i |I_i(hkl) - \langle I(hkl)\rangle| / \sum_{hkl}\sum_i I_i(hkl)$.

2.5. *Refinement*

The initial model was built using *O* (Jones *et al.*, 1991). The Cα positions from the *AMoRe* solution model were used, onto which was built the sequence of the blue-copper NiR from *P. aureofaciens* (Glocker *et al.*, 1993) using the *LEGO* commands. The sequence of PaNiR was used in view of the very high identity between all of the Cu-NiR's which have been sequenced to date and the increased identity which is expected within a sub-class; the two green NiR's have an identity of 80%, Fig. 1. Given the modest resolution, we have adopted a conservative approach in departing from the known sequence of PaNiR and variations observed in the other Cu-NiR's. The sequence of PaNiR was compared with the map and a total of 40 changes were made. These changes were all truncations, with only 12 non-alanine substitutions. Thus, the sequence used in the final model is given in Fig. 1. The model was then compared with the $2F_o - F_c$ maps, and rebuilt where necessary. The refinement was carried out in *X-PLOR* (Brünger 1992) using the Engh and Huber parameter libraries (Engh & Huber, 1991). A single cycle of simulated annealing was performed using 8–3 Å data over a temperature range 4000–300 K with a global B factor of 15 Å^2. The copper sites were restrained during simulated annealing with energies of 335 and 125 kJ mol^{-1} (80 and 30 kcal mol^{-1}) for planar and axial ligands, respectively. In order to prevent under determination non-crystallographic (NCS) restraints were used between the monomers. Strict NCS could not be applied because one of the type-2 copper ligands comes from the adjacent monomer. It is not possible to apply strict NCS in *X-PLOR* with such a geometry.

Refinements were carried out with three restraints 125, 4184 and 8368 kJ mol^{-1} (300, 1000 and 2000 kcal mol^{-1}) (125 kJ mol^{-1} being the *X-PLOR* default) which yielded essentially the same *R* factors. However, when the structural parameters were checked using *PROCHECK* (Laskowski *et al.*, 1993) the default restraints were found to give the best geometry. The initial *R* factor was 36.3% (R_{free} = 37.0%) which dropped to 21.2% (R_{free} = 27.8%) over the first cycle. In view of the limited data a conservative *B*-factor refinement was performed. The global *B* factor was initially calculated, followed by the refinement of one *B* factor per residue. The *R* factor was then 20.5% (R_{free} = 27.2%). The copper sites were then examined with respect to $2F_o - F_c$ electron-density maps and rebuilt where necessary. At this point it was noticed that the type-2 copper density was elongated and that there was well defined difference density towards the extreme of this elongation. An omit map showed this

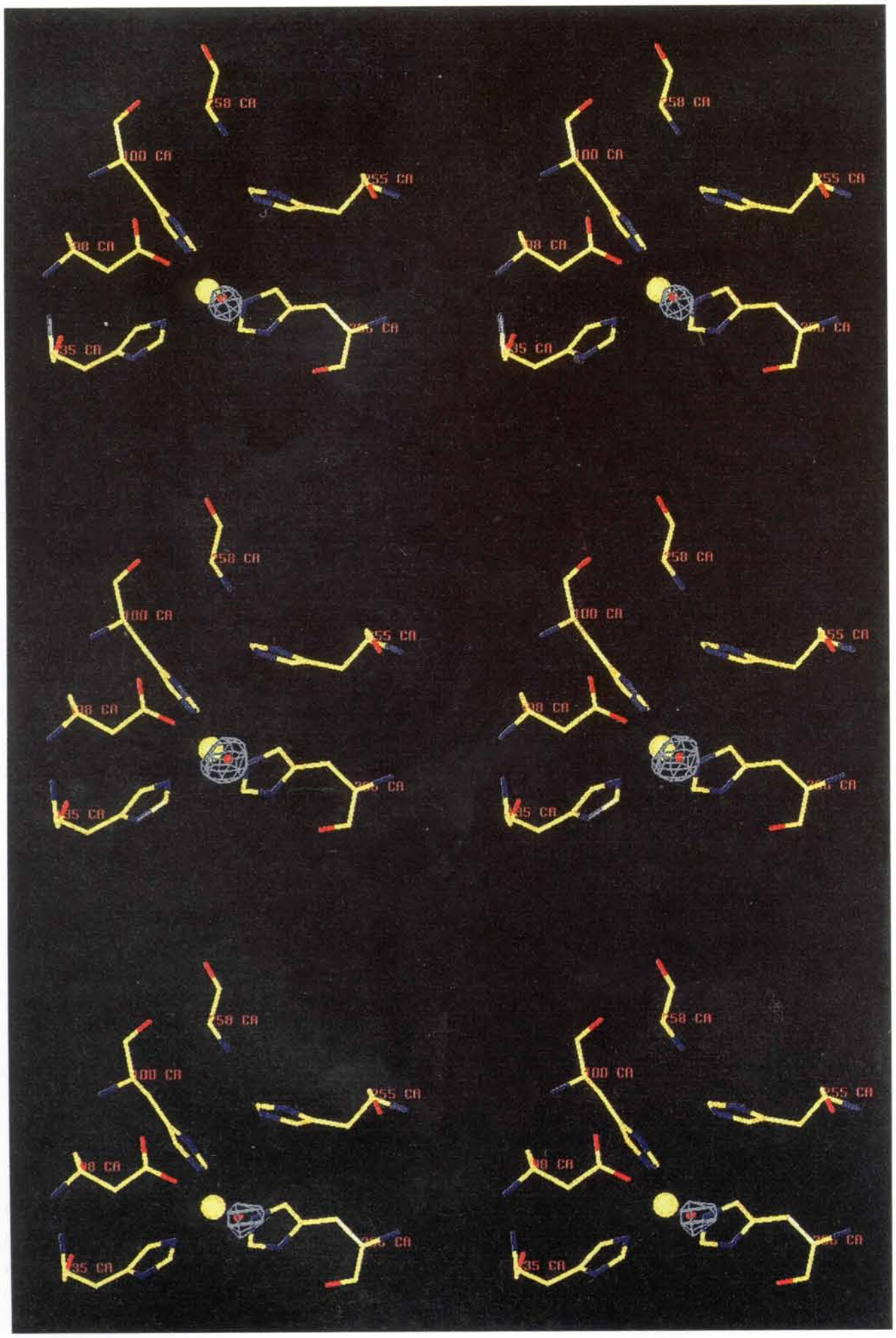

Fig. 2. Stereo plot of the type-2 Cu site for three monomers showing the difference electron density of water omit map of native AxNiR contoured at 3σ showing the water molecule above the histidine plane.

Table 2. *Summary of refinement*

(*a*) AxNiR and structural quality indicators

Cycle	*R* value	R_{free}	Atoms	Resolution range (Å)	Comments
1a	36.3→31.6	37.0→34.8	2426	8.0–3.0	*X-PLOR* prepare stage
1b	31.6→21.2	34.8→27.8	2426	8.0–3.0	Simulated annealing
1c	21.2→20.5	27.8→27.2	2426	8.0–3.0	*B*-factor refinement
2	20.4→20.0	27.2→27.0	2427	8.0–3.0	Water included, Cu rebuilt
3	20.0→20.0	27.0→27.0	2427	8.0–3.0	Cu rebuilt
4	20.0→20.3		2427	8.0–3.0	All data included

Refinement parameters	
No. of reflections	15212
No. of atoms	2427
No. of parameters	7614
R.m.s. deviations	
Bond distances (Å)	0.019
Bond angles (°)	2.9
Dihedral angles (°)	27.2
Improper angles (°)	1.7
Ramachandran plot (non-Gly and non-Pro)	
Residues in most favoured regions (%)	80.2
Residues in additional allowed regions (%)	19.0
Residues in generously allowed regions (%)	0.7
Residues in disallowed regions (%)	0.0
Structural quality	
Residues with unusual peptide orientations (%)	1.2
Resides with non-rotamer side-chain conformation (%)	13.9
Residues with poor density (real-space *R* factor > 40%) (%)	3.0
Overall *G* factor	+0.01

(*b*) Nitrite-soaked AxNiR and structural quality indicators

Cycle	*R* value	R_{free}	Atoms	Resolution range (Å)	Comments
1a	4.4→29.4	45.1→34.8	2426	8.0–2.8	*X-PLOR* prepare stage
1b	29.4→25.7	34.8→30.2	2426	8.0–2.8	Simulated annealing
1c	25.7→23.6	30.2→27.9	2426	8.0–2.8	*B*-factor refinement
2	23.6→23.6	27.9→27.9	2429	8.0–2.8	NO_2 included, Cu rebuilt
3	23.6→23.5	27.9→27.9	2430	8.0–2.8	NO_2 and Cu rebuilt, water included.
4	23.5→23.6		2430	8.0–2.8	All data included

Refinement parameters	
No. of reflections	22971
No. of atoms	2430
No. of parameters	7624
R.m.s. deviations	
Bond distances (Å)	0.022
Bond angles (°)	2.8
Dihedral angles (°)	27.4
Improper angles (°)	1.5
Ramachandran plot (non-Gly and non-Pro)	
Residues in most favoured regions (%)	85.7
Residues in addtional allowed regions (%)	13.9
Residues in generously allowed regions (%)	0.4
Residues in disallowed regions (%)	0.0
Structural quality	
Residues with unusual peptide orientations (%)	1.5
Residues with non-rotamer side-chain conformation (%)	10.6
Residues with poor density (real-space *R* factor > 40%) (%)	2.1
Overall *G* factor	+0.08

density to be spherical fully consistent with the ligation of a water molecule to Cu as shown in Fig. 2 for the three monomers. A further 40 cycles of positional refinement were then carried out with the copper restraints removed. This yielded an *R* factor of 20.0% (R_{free} = 27.0%), with no significant changes in the copper–ligand distances. The entire data set, including the reflections which were set aside for calculating R_{free}, was then used in a 40 cycles of positional refinement which yielded a final *R* factor of 20.3% (Table 2).

Refinement of nitrite-soaked AxNiR crystal was carried out using the same starting model and protocol as for the native AxNiR. In the initial simulated-annealing cycle the *R* factor started at 44.4% (R_{free} = 45.1%) which dropped to 25.7% (R_{free} = 30.2%). *B*-factor refinement reduced the residuals to 24.1% (R_{free} = 28.1%) and with further positional refinement to 23.6% (R_{free} = 27.9%). Density extension was again observed at the type-2 copper site but to a greater extent. There was also a large difference density in the omit map at this point. This density was at least twice as large as that for the native structure water molecule, as well as being elongated compatible with the presence of a nitrite molecule. In addition, the location of this density was different from the water density of the native structure *i.e.* the centre of the water density in native structure was at the edge of this density. A nitrite molecule was built into this density to lie along the direction of elongation, Fig. 3. A second region of positive density, consistent with a water molecule, was observed in the $2F_o - F_c$ map between Asp98 and His255 in a position similar to that suggested by modelling studies (Strange *et al.*, 1995). There was again significant difference density at this point which was assigned to a water molecule. No other density was observed in the Cu cavity at this stage. One cycle of *B*-factor refinement was performed with one *B* value per residue including one for the nitrite molecule. The entire data set, including the reflections which were set aside for calculating R_{free}, was then used in a 40 cycles of positional refinement which yielded a final *R* factor of 23.6%.

3. Results and discussion

3.1. *The overall structure*

The native model consists of 330 residues, two Cu atoms and one water molecule (density of residues 1–10 is not visible) per monomer. The r.m.s. deviation between the monomers using restrained NCS is 0.05 Å. The final crystallographic *R* factor was 20.3%. The

Ramachandran plot (Fig. 4) shows 80.2% of the residues in most favoured regions and 19.0% of the residues in additional allowed regions. The average *B* factor of the monomer is 15 Å^2, with the maximum being 79.1 Å^2 at the C terminal. The nitrite-soaked model shows 85.7% of the residues in most favoured regions and 13.9% of the residues in additional allowed regions. The average *B* factor of the molecules is unexpectedly low at 10.9 Å^2, with the maximum being 74.3 Å^2 at the C terminal.

The overall structure of AxNiR is trimeric, with each crystallographic asymmetric unit containing one trimer (Fig. 5). The majority of the monomer of AxNiR consists of two eight-stranded β-barrel domains (domain I, residues 11–160; domain II, residues 161–340). Each domain I interacts with domain II of the adjacent monomer providing the bulk of the inter-monomer contacts. There are also interactions between the domains II in adjacent monomers close to the threefold axis.

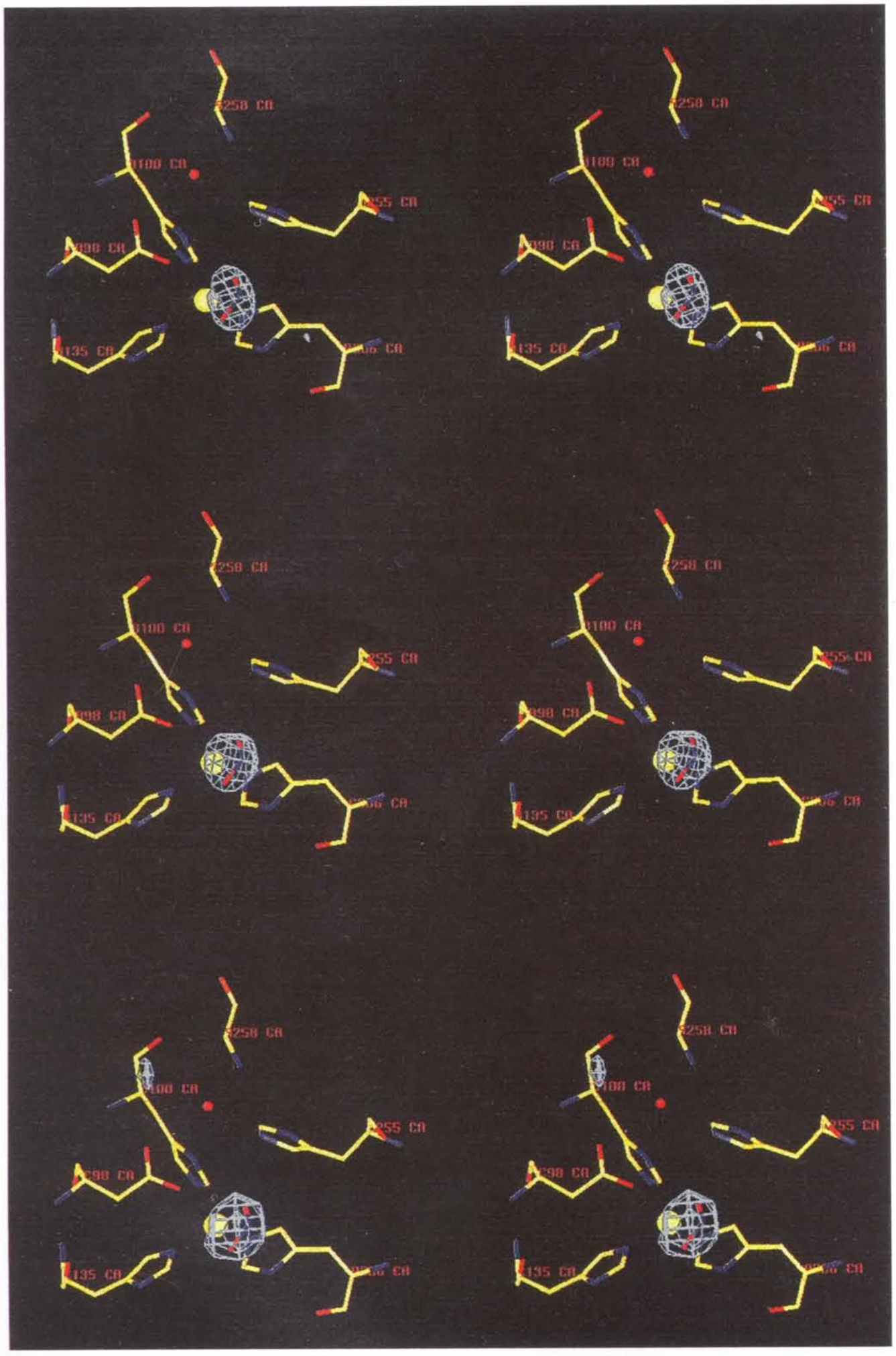

Fig. 3. Stereo plot of the difference electron density of nitrite omit map of nitrite soaked AxNiR contoured at 3σ showing the elongated electron density of the nitrite molecule for the three monomers. Nitrite had full occupancy and *B* refined to 29 Å^2. The position of a water molecule (red cross) is also shown.

The C terminal of the monomer forms an arm (residues 323–340) extending to the outer edge of the adjacent monomers domain I forming contacts with residues in the region 100–125.

3.2. *The copper sites*

The AxNiR monomer contains two Cu atoms which form one type-1 and one type-2 copper site. The two Cu atoms are 12.6 Å apart. They are connected directly by residues Cys136 and His135. The $2F_o - F_c$ electron density of the two sites contoured at 1σ is shown in Fig. 6.

The type-1 copper is ligated by two His, one Cys and one Met residues in a distorted trigonal planar geometry. The three strong planar ligands are His95 $N^{\delta 1}$, Cys136 S^{γ} and His145 $N^{\delta 1}$, while Met150 S^{δ} is in an axial position. The copper-to-ligand distances in the native structure are ~1.9, 2.0, 2.0 and 2.6 Å, respectively (2.1, 2.1, 2.0 and 2.7 Å in the nitrite-soaked structure). The fifth ligand seen in the azurin structures (the Gly45 carbonyl O atom) (Baker, 1988; Dodd, Hasnain, Abraham *et al.*, 1995; Nar, Messerschmidt, Huber, van de Kamp & Canters, 1991) is present in AxNiR but, at 3.7 Å, is too distant to interact with Cu. The geometry of the site is similar to that of AfNiR and that of azurin II from *A. xylosoxidans* (Fig. 7). The copper ligand His145 is orientated similarly to the corresponding His117 in azurin II which has its $N^{\varepsilon 2}$ atom exposed to the solvent (Dodd, Hasnain, Abraham *et al.*, 1995). The type-1 copper lies ~4 Å from the protein surface. The Cu–ligand distances are very similar to those known for other type-1 Cu centres in proteins such as azurin and plastocyanin except the Cu–Smet distance is substantially shorter. The Cu–Smet distance is the same as found in the crystallographic structures of the two green NiR's. XAFS studies had suggested that in view of the close resemblance of the data for T_2DAxNiR and azurin, the Cu–Smet may be longer than the green NiR's and similar to azurin. However, we note that the contribution of Cu–Smet has been difficult to establish in small blue-copper proteins by XAFS (Scott, Hahn, Doniach, Freeman & Hodgson, 1982; Murphy *et al.*, 1993).

The type-2 Cu site lies in a ~13 Å deep cleft between domain I and domain II of adjacent monomers where it is directly exposed to the solvent. This copper is ligated by His100, His135 from domain I of one monomer while the third ligand (His306) is from domain II of the adjacent monomer. The copper-to-ligand distances in the native structure are 2.1, 2.1 and 2.0 Å, respectively (2.2, 2.1 and 2.0 Å, in the nitrite-soaked structure). All three histidines ligate the copper *via* their $N^{\varepsilon 2}$ atoms. The residues His100 and His306 have their $N^{\delta 1}$ atom hydrogen bonded to their respective carbonyl O atoms. The geometry of the site is again similar to that of AfNiR

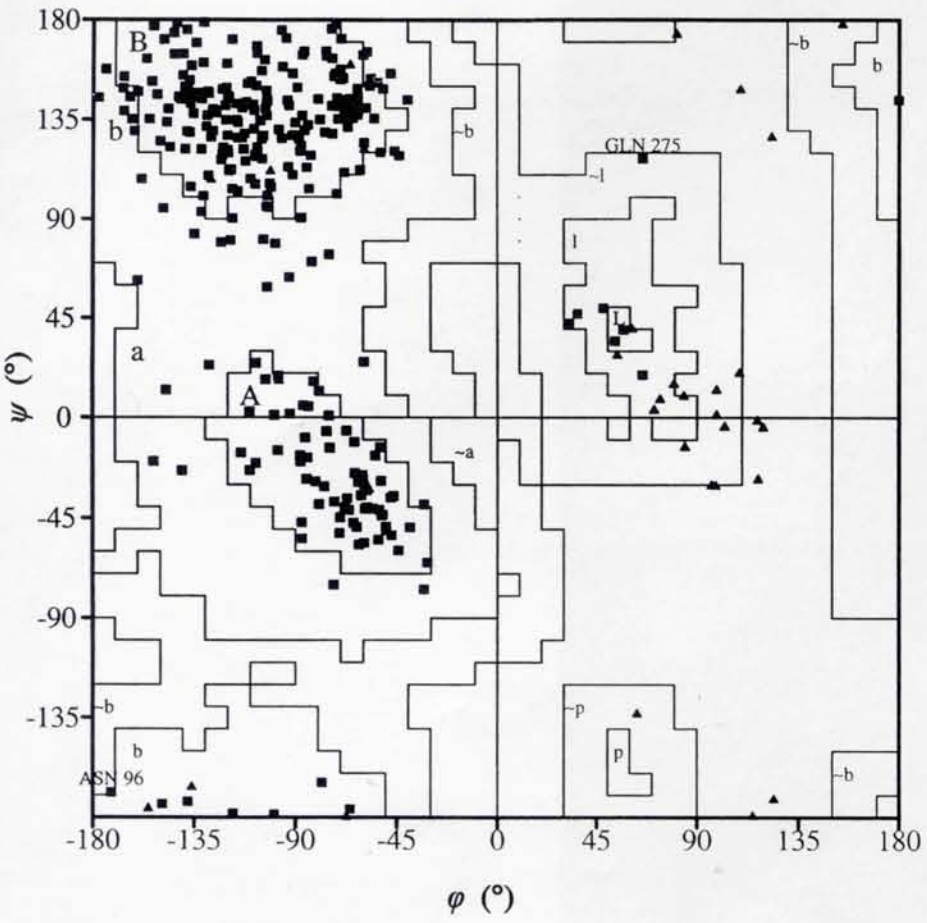

Fig. 4. The Ramachandran plot of native AxNiR from *PROCHECK* (Laskowski *et al.*, 1993).

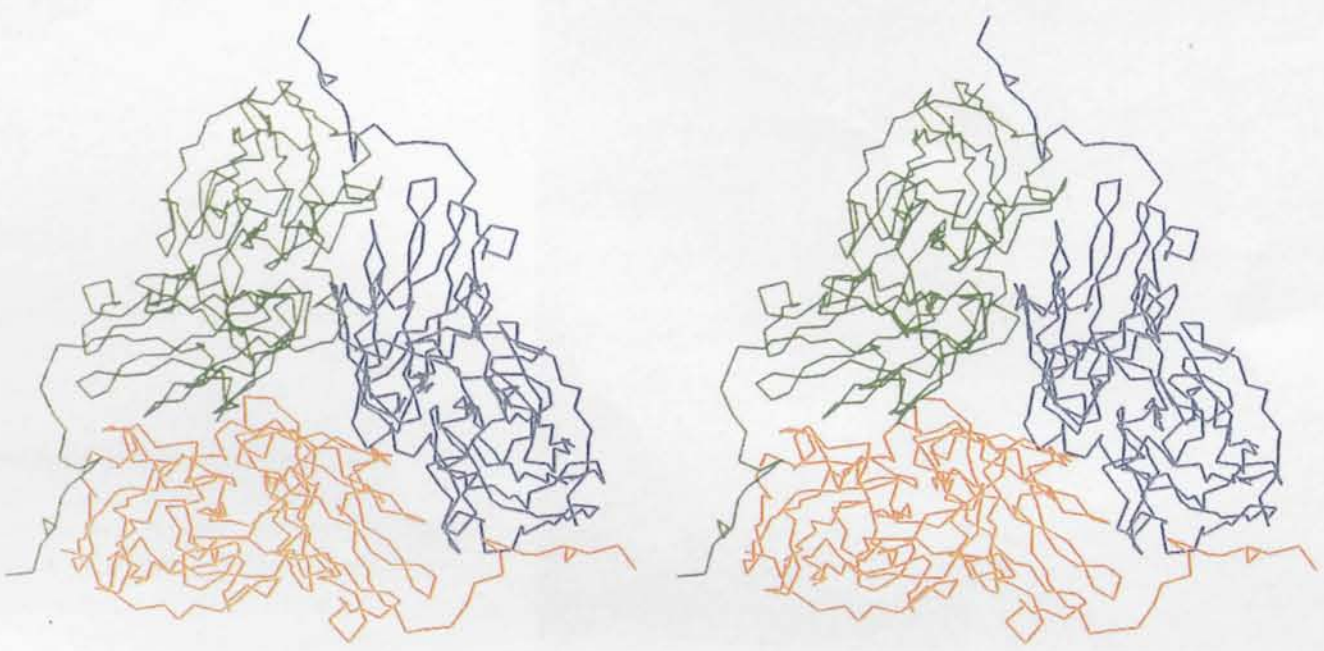

Fig. 5. The structure of the trimer of native AxNiR showing the twin β-barrel fold of the monomers. The Cu atoms and the ligated waters are shown as blue and white spheres, respectively.

and AcNiR (Fig. 8). Two other residues, Asp98 and His 255, of potential importance in the binding of nitrite to the type-2 copper are found to be in similar positions to those in AfNiR and AcNiR. In addition there is well defined spherical difference density above the plane of the histidine ligands. This density is attributed to a water molecule which is observed in the other NiR structures to some extent. The distance of the water molecule at ~1.7 Å from the copper is in good agreement with the XAFS results (Strange *et al.*, 1995) given the expected accuracy of these crystallographic studies to be no better than 0.2 Å for metrical information.

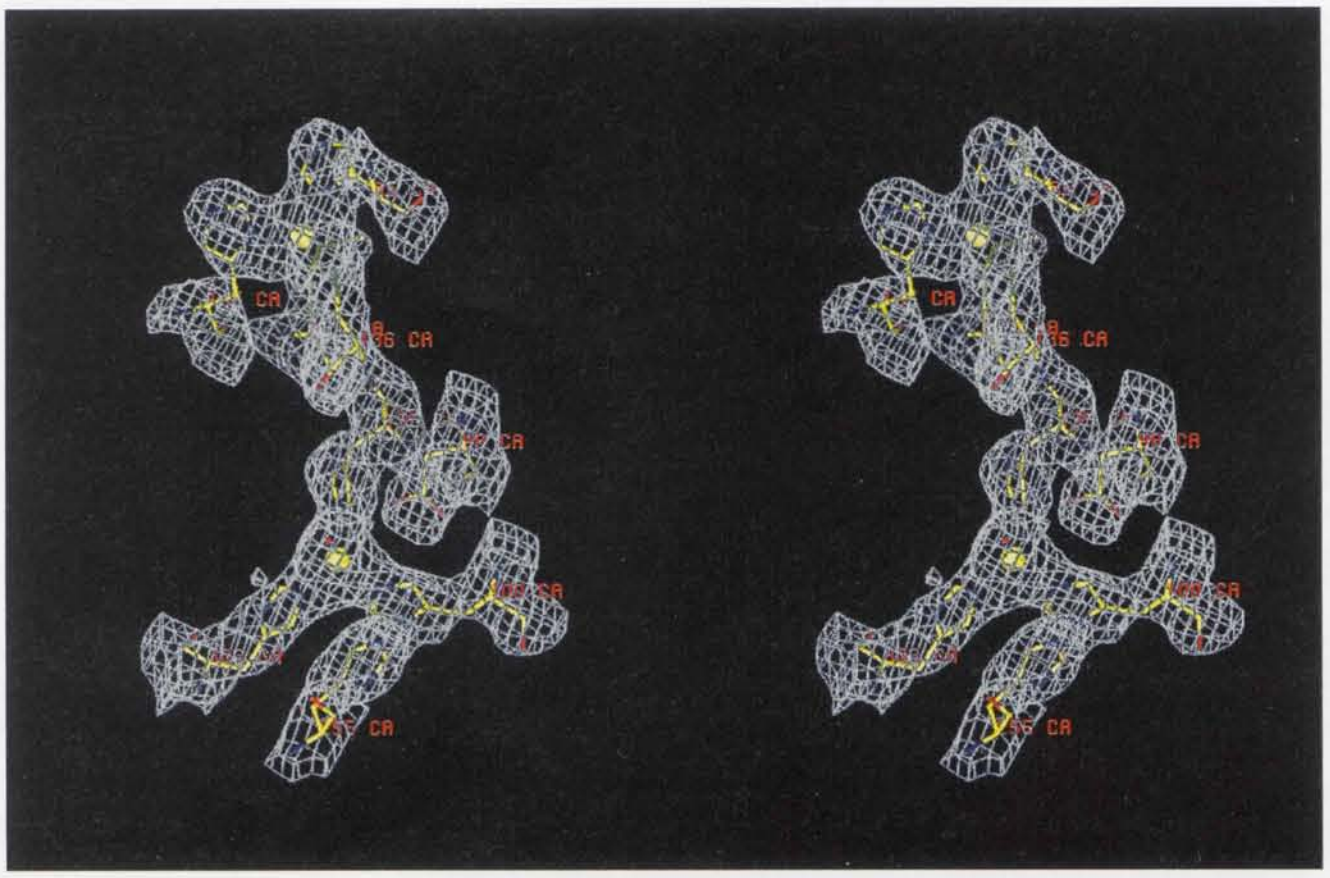

Fig. 6. Stereo plot of the $2F_{obs} - F_{calc}$ electron density of the two copper sites of native AxNiR contoured at 1σ.

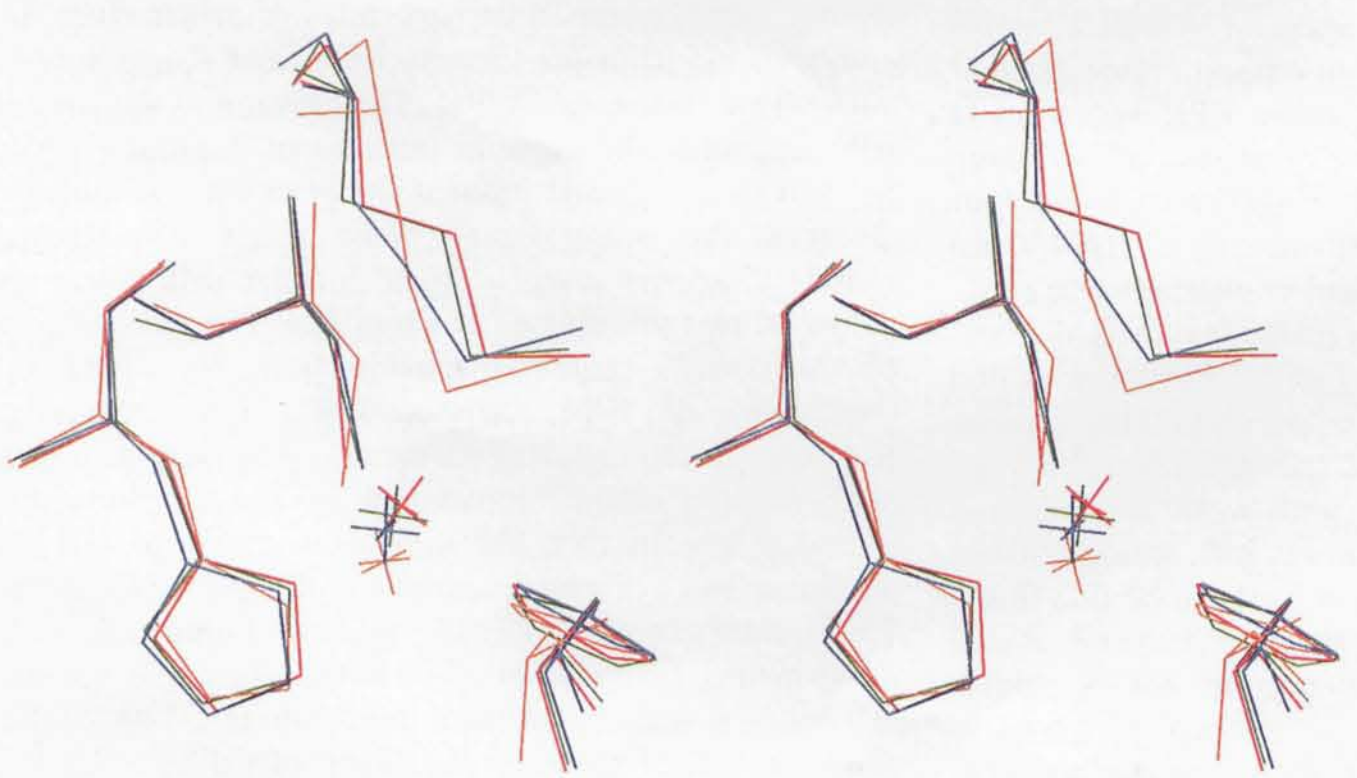

Fig. 7. Superposition of the type-1 sites of native AxNiR (blue), AfNiR (green), AcNiR (red) and AzII (orange) showing the relative positions of the Cu atom with repect to the plane formed by the strong ligands. The superposition was carried out on the three strongly ligating residues; namely His95, His145 and Cys136.

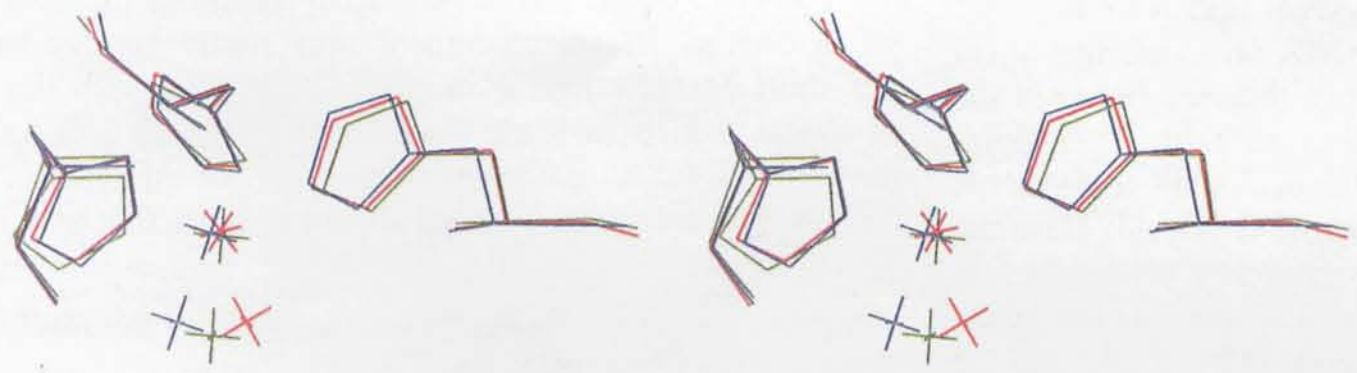

Fig. 8. Superposition of the type-2 sites of native AxNiR (blue), AfNiR (green), AcNiR (red). The variability in the position of the water molecule is clearly seen. The superposition was carried out on the three ligating histidine residues and the copper.

Table 3. *Details of the copper geometry of native (3 Å resolution) and nitrite-soaked AxNiR (2.8 Å) compared with those of AfNiR (2.6 Å), AcNiR (2.1 Å), AcNiR + nitrite (2.3 Å) and azurin II (1.9 Å)*

Accuracy of metal–ligand distances in crystallographic structures at these resolutions is expected to be $\simeq 0.2$ Å. Metrical information for the catalytic Cu is included from XAFS study (Strange *et al.*, 1995) for comparison, these are expected to be ± 0.02 Å for inner ligands while the longer O distance from nitrite is ill defined because of its distant location and overlap of its scattering contribution with those from outer C atoms of imidazole groups.

Cu ligand	AxNiR	AxNiR+Nit	AxNir (*a*) (exafs)	AxNiR+Nit (exafs) (*a*)	AfNiR (*b*)	AcNiR (*c*)	AcNiR+Nit (*c*)	AzII (*d*)
Type1Cu								
95 $N^{\delta 1}$	1.87	2.14			2.13	2.02	2.02	2.02 (45 $N^{\delta 1}$)
145 $N^{\delta 1}$	1.96	1.99			1.97	2.02	2.03	2.02 (117 $N^{\delta 1}$)
136 S^{γ}	2.03	2.07			2.19	2.16	2.24	2.12 (112 S^{γ})
150 S^{δ}	2.59	2.66			2.59	2.59	2.56	3.26 (121 S^{δ})
Type 2 Cu								
100 $N^{\epsilon 2}$	2.08	2.16	1.95	2.03	2.08	2.00	2.07	
135 $N^{\epsilon 2}$	2.09	2.00	1.95	2.03	2.32	2.04	2.10	
306 $N^{\epsilon 2}$	1.96	2.15	1.95	2.03	2.00	2.19	2.16	
Wat	1.70		1.98		1.85	1.66		
Nit:O1		1.73		1.95			2.16	
Nit:O2		2.37		2.85			2.53	

References: (*a*) Strange *et al.* (1995). (*b*) Kukimoto *et al.* (1994). (*c*) Adman *et al.* (1995). (*d*) Dodd, Hasnain, Abraham *et al.* (1995).

3.3. *Comparison of Cu sites in AxNiR with green NiR's*

The structure of AxNiR is very similar to AfNiR and AcNiR. The r.m.s. deviation in the Cα positions between AxNiR and AfNiR and AcNiR is 0.60 and 0.67 Å, respectively.

The spectroscopic properties of proteins containing type-1 Cu centres have attracted much attention for structural and site-directed mutagenesis studies. Proteins containing type-1 Cu centres can exhibit either axial or rhombic EPR spectra. The rhombic EPR spectrum is accompanied by the appearance of a band at ~450 nm in addition to the optical band at ~600 nm. The colour of the protein changes when the intensity of the 450 nm becomes significant. Valentine and co-workers (Lu *et al.*, 1993; Han *et al.*, 1993) have suggested that there is a correlation between the rhombocity of the EPR spectra and the ratio of the intensities of the 450 and 600 nm bands. They have also suggested that the difference between 'classical' blue-copper proteins with weak 450 nm band and the 'green' blue-copper proteins with strong 450 nm as observed in the green NiR's is likely to be due to the strength of the Cu—*L* bond of the fourth ligand. Based on the reported Cu—S^{δ} distance from XAFS studies (~3 Å) and the observed Cu—S^{δ} distance (~2.6 Å) in AcNiR, Adman *et al.* (1995) suggested that this apparent difference in distances might be correlated with the difference in colour between AxNiR and AcNiR.

It is now clear from the AxNiR structure that there is no difference in the Cu—Smet distance between the AxNiR and the two green NiR's (see Table 3). A comparison of the type-1 copper sites of AxNiR and AcNiR with those from AfNiR and azurin II (Dodd, Hasnain, Abraham *et al.*, 1995) show significant differences in the position of the Cu atom with respect to the plane formed by the three strong ligands (Fig. 7). In AxNiR the Cu atom is out of this plane by ≤ 0.2 Å,* whereas in the cases of green AfNiR and AcNiR copper is displaced by ~0.5 and 0.6 Å, respectively. In azurin II from this organism whose structure is now known to 1.75 Å (Dodd & Hasnain, unpublished results), the Cu atom is essentially in the plane with the deviation being 0.02 Å. Cu is also found to be within ~0.1 Å of the strong ligands plane in the structures of azurin from *Alcaligenes denitrificans* (Baker, 1988) and *Pseudomonas aeruginosa* (Nar *et al.*, 1991). The location of the copper with respect to the plane in the case of the blue AxNiR is, therefore, of some interest. Its position significantly closer to the strong ligand plane and similar to that found in azurins may account for the differences in colour of two sub-classes of Cu-NiR's. The green colour of the Glu121 mutant of azurin from *P. aeruginosa* (Karlsson *et al.*, 1991; Karlsson, 1993; Strange, Murphy, Karlsson, Reinhammar & Hasnain, 1996) may also thus arise from a similar movement of the Cu from the ligand plane. In fact, the crystal structure of Glu121 mutant shows a displacement of Cu of ~0.4 Å (Karlsson, 1993). Furthermore, a Gln121 mutant of azurin from *A. denitrificans* (Romero *et al.*, 1991), where the 450 nm is observed with significant intensity ($\varepsilon \simeq 1200$), also shows an out-of-plane displacement of Cu by ~0.3 Å.

However, it is unclear why Cu is out of plane in the case of NiR's and substantially more in the case green NiR's. The displacement may partly be due to the short Met150 ligand in NiR's compared with that of azurin which in itself may result from the lack of (or much weaker) carbonyl interaction. In AfNiR and AcNiR the carbonyl O atom distance from Cu is 4.2

* We note that at this resolution (2.8–3.0 Å) this is not significantly different from Cu being in the plane.

and 4.3 Å, respectively, compared with 3.7 Å in the AxNiR structure. This difference may arise from the non-conserved nature of the residue 94 providing the carbonyl O atom. The distance between the carbonyl O atom and Cu is too large for this interaction to have a covalent character, but the electrostatic interaction is likely to be significant as is the case for azurins (Canters & Gilardi, 1993). It has been suggested that the presence of this interaction in azurin helps to stabilize the Met121 mutants in azurins compared to poor success in its counterpart in plastocyanin (Adman, 1991). A comparison of the AxNiR structure with that of azurin II (Dodd, Hasnain, Abraham *et al.*, 1995) shows the Met ligand to be in almost identical conformation but displaced laterally by a distance of ~0.9 Å resulting in a shortening of Cu–Smet distance to 2.6 Å compared with 3.26 Å, see Table 3. The orientation of Met in the two green NiR's appears to be different from that observed in azurin II and AxNiR, Fig. 7. The significantly shorter Cu–Smet distance of the three crystallographically characterized NiR's, including AxNiR compared to azurins is similar to pseudo-azurin and cucumber basic blue protein and we suggest that the distance of this methionine in itself is not responsible for the differences in colour. We propose that, among other factors, the position of Cu with respect to the N_2S plane most likely results from a subtle balance between the two axial interactions and that the extent of the 'out-of-plane' movement of Cu changes the Cu centre from a blue to green.

3.4. *Nitrite binding*

Unlike haem-based NiR's, very limited mechanistic work has been performed on Cu-NiR's and details of the enzymatic cycle are not defined. We envisage the following reaction scheme for Cu-NiR's, the complex for which structural details are provided here is highlighted in the scheme given below.

EPR and ENDOR studies (Howes *et al.*, 1994) of AxNiR have shown that the type-1 Cu site is essentially unperturbed upon the addition of nitrite to the type-2 Cu-deficient enzyme and that nitrite binding effects the 'type-2' Cu site. On the basis of $^{14}N,^{15}N$ ENDOR, Howes *et al.* argue in favour of extensive effect on type-2 Cu ligation upon substrate binding rather than simply the substitution of an apical water molecule by the substrate. Adman *et al.* (1995) have reported a reanalysis of their preliminary soaking experiment of AcNiR crystals. Even though the interpretation of this (the only) crystallographic study of NiR—NO_2 complex is somewhat complicated by the fact that the type-2 Cu site does not have a 'full' occupancy in the soaked crystals and only 50% of them have nitrite (the remainder presumably still have bound water), it is suggested that a substitution of water by the substrate takes place without any rearrangement of the type-2 Cu ligands. However, EXAFS data for AxNiR show that nitrite binding is accompanied by expansion of the copper coordination sphere (Strange *et al.*, 1995).

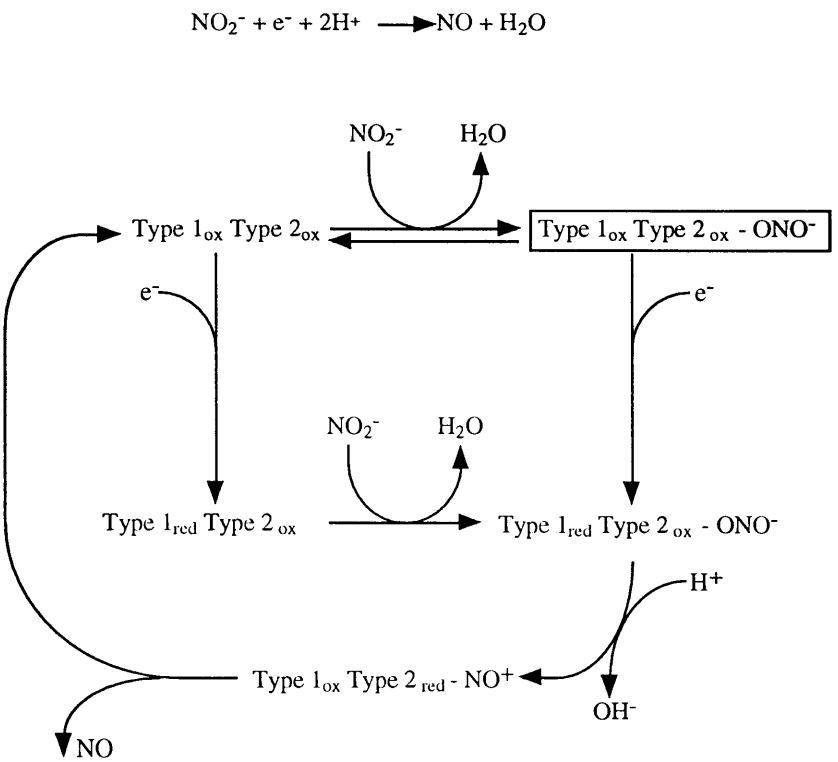

In the nitrite-soaked AxNiR structure, the nitrite density is found ~1 Å away from the water molecule in the native protein. The nitrite ligates the copper in a bidentate fashion with the copper to nitrite O atom distances being ~1.7 and 2.4 Å. The nitrite is oriented such that hydrogen bonding occurs between the second O atom and the $O^{\delta 1}$ of Asp98 at a distance of ~3.4 Å. The nitrite is found to be rotated by 90° with respect to the position suggested by modelling studies (Strange *et al.*, 1995) such that hydrogen bonding to the $N^{\varepsilon 2}$ of His255 is not possible. Upon nitrite binding, the position of the Asp98 changes by ~0.3 Å away from the type-2 Cu atom. There is no significant change in the Cu–ligand distances for both Cu site except at the type-1 Cu, the Cu–$N^{\delta 1}$ (His95) distance is increased by ~0.3 Å, Fig. 9. The water molecule found near the type-2 copper site is hydrogen bonded to the other Asp98 terminal O atom at a distance of ~3.2 Å and to the amide N atom of Gly258 at ~2.9 Å. The third potential hydrogen-bonding position is to the $N^{\varepsilon 2}$ of His255 at a distance of ~3.5 Å (Fig. 10).

3.5. *Proposed mechanism*

The bidentate mode for nitrite binding to AxNiR reported here is similar to that reported by Adman *et al.* (1995) for AcNiR. We recently proposed a mechanism of nitrite reduction by AxNiR based on an XAFS and modelling study (Strange *et al.*, 1995). Further refinement can take place in view of the direct observation of bound nitrite and a water molecule in the nitrite-soaked AxNiR crystals. The mechanism for nitrite reduction thus involves the displacement of the bound water molecule at the type-2 Cu by nitrite to form a Cu^{2+}–NO^{2-} complex. The displaced water leaves as an OH^- leaving Asp98 protonated. The type-1 Cu accepts an electron from the donor which is transferred to type-2 Cu. The cleavage of the O—N bond in nitrite is facilitated by the reduction of the type-2 Cu and donation of a proton from Asp98, such that the cleaved oxygen leaves as a OH^-. This OH^- then picks up a proton to form a water molecule, leaving the type-2 Cu reduced with an NO^+ bound. The NO moiety bound to the Cu atom then undergoes a linkage isomerism (O to N) forming a copper-nitrosyl intermediate Cu^I—N—NO^+. Liberation of the NO by replacement with a water molecule and the consequent oxidation of the Cu atom restores the enzyme to its initial state ready for subsequent turnover cycles.

The proposed Cu-nitrosyl intermediate (Hulse, Averill & Tiedje, 1989) has not been directly observed in enzyme turnover of Cu-containing NiR's, in contrast to heme NiR where Fourier transform infra-red (FTIR) spectroscopy has detected such a species (Wang, & Averill, 1996). However, studies on the reactivity of synthetic mononuclear Cu^{II} complexes (Cassella, Carugo, Gullotti, Doldi & Frassoni, 1996) of O-bonded nitrite adducts has shown that the rates of protonation and dehydration of these compounds are faster than their rates of reduction to form NO. Thus, studies of these mimetic systems are consistent with the proposal that the reduction of nitrite by Cu-containing NiR proceeds *via* such a nitrosyl intermediate.

Further evidence for this intermediate, and for it having a significant lifetime, is provided by the formation of N_2O as a minor product during the turnover of AcNiR. It has been suggested that the reaction of NO, generated during turnover as a product of the reduction of nitrite, reacts with the putative copper-nitrosyl intermediate (Jackson, Tiedje & Averill, 1991) to form N_2O. In the case of AcNiR the putative E—NO^+ has been trapped in the presence of NH_2OH, and the production of N_2O has been demonstrated *via* this intermediate (Hulse *et*

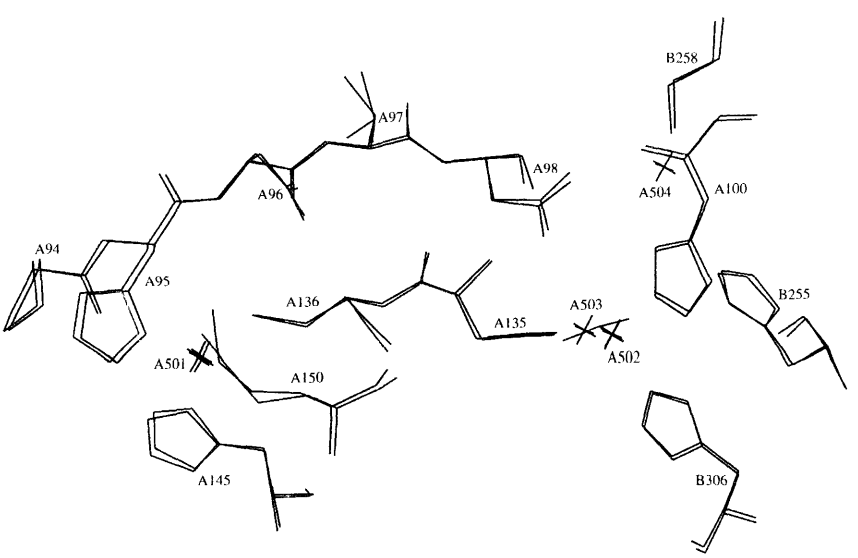

Fig. 9. Superposition of native (blue) and nitrite-soaked (red) AxNiR structures around the Cu sites. The superposition was carried out on all ligating residues and the two Cu atoms.

al., 1989). Adman *et al.* (1995) have put forward an alternative proposal for the mechanism where following cleavage of an O—N bond of nitrite, the release of NO occurs before release of the second O atom, which remains bound to the Cu atom. In this scheme, where the lifetime of any Cu^{I}–NO^{+} species is likely to be shorter than in our proposed mechanism it is more difficult to reconcile the formation of N_2O *via* the intermediate.

XAFS data had shown that the Cu–ligand distances increase by ~0.08 Å upon nitrite binding. The reason for this is clear now from the nitrite soaked AxNiR crystallographic structure in that the coordination number at the Cu site has increased to five. It is well known from chemical compounds that the Cu-ligand distance increase by approximately this amount when the coordination number is increased by one for the same oxidation state of Cu. The increased coordination due to asymmetric bidentate binding of nitrite at the type-2 Cu site will result in the expansion of the strong Cu–His distances. In XAFS, the O atom at the longer distance of ~2.4 Å is not expected to make a strong contribution. In crystallographic structures at 2–3 Å resolution, differences in metal–ligand distances of ~0.1 Å cannot be observed with any confidence as the accuracy of metrical information from such structures is expected to be ~0.2 Å.

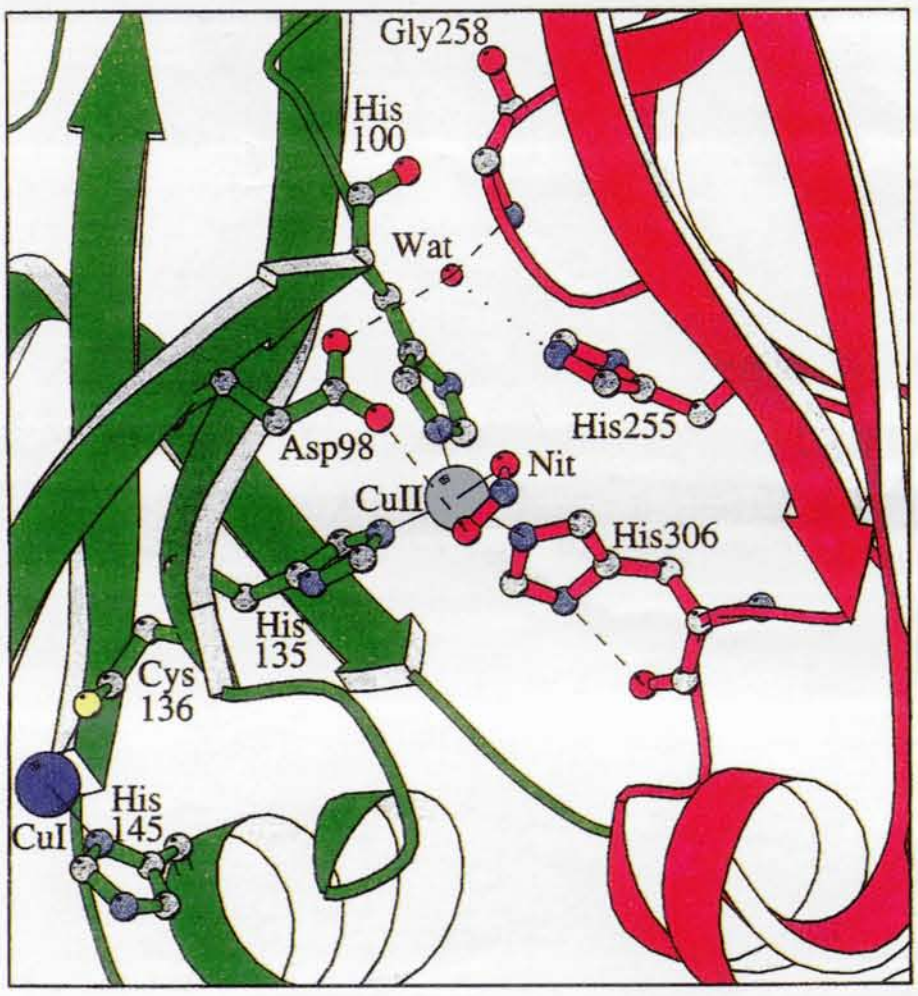

Fig. 10. The mode of nitrite binding to type-2 Cu (denoted by CuII) at the subunit interface in nitrite reductase (the two monomers are depicted by red and green colour). The nitrite is bound to the copper in a bidentate manner. The only possible hydrogen bonding of the nitrite to Asp98 is shown. The water molecule is hydrogen bonded by Asp98 and Gly258, with the potential for bonding (shown as dots) to His255 $N^{\varepsilon 2}$. This figure was produced using *MOLSCRIPT* (Kraulis, 1991).

Thus, there are some parallels in nitrite reduction in haem *cd*1 NiR's and Cu-NiR, *e.g.* for the formation of N_2O as a product under some conditions, the location of the catalytic site at the domain interface (Fülop, Moir, Ferguson & Hajdu, 1995). However, for cytochrome *cd*1, it has been recently suggested that NO, which has high affinity to Fe is forced out from the haem d1 pocket through a large scale domain movement which takes place upon reduction (Fülop *et al.*, 1995). In the case of Cu-NiR's, domain interface seem to remain intact even in the absence of the catalytic Cu suggesting that the catalytic pocket is rigorously configured. It may thus be the unusual Cu site, which has already been noted (Strange *et al.*, 1995) to resemble the Zn site in carbonic anhydrase, which could facilitate release of NO which has high affinity for type-2 Cu centres. Further higher resolution studies of the two classes of nitrite reductase are required together with mechanistic studies before a definitive mechanism for nitrite reduction and NO release can be established.

This work benefitted from the use of the SEQNET facility. We are grateful to our colleagues, in particular to Drs Gunter Grossmann, Richard Strange and Ian Harvey for their interest in the project. We also would like to thank Professor Sakabe and Dr Watanabe for their help and hospitality at the Photon Factory. We are grateful to Drs Liz Duke and Colin Nave for their help and interest. We would like to thank the referees for their helpful comments.*

* Atomic coordinates and structure factors have been deposited with the Protein Data Bank, Brookhaven National Laboratory (Reference: INDS, R1INDSSF). Free copies may be obtained through The Managing Editor, International Union of Crystallography, 5 Abbey Square, Chester CH1 2HU, England (Reference: HE0184).

References

Abraham, Z. H. L., Lowe, D. J. & Smith, B. E. (1993). *Biochem. J.* **295**, 587–593.

Adman, E. T. (1991). *Adv. Protein Chem.* **42**, 145–197.

Adman, E. T., Godden, J. E. & Turley, S. (1995). *J. Biol. Chem.* **270**, 27458–27474.

Adman, E. T., Turley, S., Bramson, R. Petratos, K., Banner, D., Tsernoglous, D., Beppu, T. & Watanabe, H. (1989). *J. Biol. Chem.* **264**, 87–99

Baker, E. N. (1988). *J. Mol. Biol.* **203**, 1071–1095.

Brünger, A. T. (1992). *X-PLOR Manual*, Version 3.0, Yale University, New Haven, Connecticut, USA.

Canters, G. W. & Gilardi, G. (1993). *FEBS Lett.* **325**, 39–48.

Cassella, L, Carugo, O, Gullotti, M, Doldi, S. & Frassoni, M. (1996). *Inorg. Chem.* **35**, 1101–1113

Collaborative Computational Project, Number 4 (1994). *Acta Cryst.* D**50**, 760–763.

Dodd, F., Grossmann, G., Abraham, Z., Murphy, L., Smith, B. E., Eady, R. R., Nishiyama, M., Beppu, T., Adman, E. T. & Hasnain, S. S. (1993). Daresbury Laboratory Annual Report 1992/93, p. 221.

Dodd, F. E., Hasnain, S. S., Abraham, Z. H. L., Eady R. R. & Smith, B. E. (1995). *Acta Cryst.* **D51**, 1052–1064.

Dodd, F. E., Hasnain, S. S., Hunter, W. N., Abraham, Z. H. L., Debenham, M., Kanzler, H., Eldridge, M., Eady, R. R., Ambler, R. P. & Smith, B. E. (1995) *Biochemistry*, **34**, 10180–10186

Engh, R. A. & Huber, R. (1991). *Acta Cryst.* A**47**, 392–400.

Fenderson, F. F., Kumar, S., Adman, E. T., Lui, M. Y., Payne, W. J. & LeGall, J. (1986). *Biochenistry*, **30**, 7180–7185.

Fülop, V., Moir, J. W. B., Ferguson, S. J. & Hajdu, J. (1995). *Cell*, **81**, 369–377.

Glocker, A. B., Jüngst, A. & Zumft, W. G. (1993). *Arch. Microbiol.* **160**, 18–26.

Godden, J. W., Turley, S., Teller, D. C., Adman, E. T., Liu, M. Y., Payne, W. J. & LeGall, J. (1991). *Science*, **253**, 438–442.

Grossmann, J. G., Abraham, Z. H. L., Adman, E. T., Neu, M., Eady, R. R., Smith, B. E. & Hasnain, S. S. (1993). *Biochemistry*, **32**, 7360–7366.

Han, J., Loehr, T. M., Lu, Y., Valentine, J. S., Averill, B. A. & Sanders-Loehr, (1993). *J. Am. Chem. Soc.* **115**, 4256–4263.

Higashi, T. (1989). *J. Appl. Cryst.* **22**, 9–18.

Higgins, D. G., Bleasby, A. J. & Fuchs, R. (1992). *CABIOS*, **8**, 189–191

Howes, B. D., Abraham, Z. H. L., Lowe, D. J. & Brüser, T., Eady, R. R. & Smith, B. E. (1994). *Biochemistry*, **33**, 3171–3177.

Hulse, C. L., Averill, B. A. & Tiedje, J. M., (1989). *J. Am. Chem. Soc.* **111**, 2322–2323.

Jackson, M. A. Tiedje, J. M. & Averill, B. A. (1991). *FEBS Lett.* **291**, 41–44

Jones, T. A., Zou, J. Y., Cowan, S. W. & Kjeldgaard, M. (1991). *Acta Cryst.* A**47**, 110–119.

Kakutani, T., Watanabe, H., Arima, K. & Beppu, T. (1981). *J. Biochem.* **89**, 463–472.

Karlsson, G. (1993). PhD thesis, University of Goteborg, Sweden.

Karlsson, B. G., Nordling, M., Pascher, T., Tsai, L.-C., Sjölin, L. & Lundberg, L. G. (1991). Journal?? **4**(3), 343–349.

Kraulis, P. J. (1991). *J. Appl. Cryst.* **24**, 946–950.

Kukimoto, M., Nishiyama, M,. Murphy, M. E. P., Turley, S., Adman, E. T., Horinouchi, S. & Beppu, T. (1994). *Biochemistry*, **33**, 5246–5252.

Laskowski, R. A., MacArthur, M. W., Moss, D. S. & Thornton, J. M. (1993). *J. Appl. Cryst.* **25**, 283–291.

Libby, E. & Averill, B. A. (1992). *Biochem. Biophys. Res. Commun.* **187**, 1529–1535.

Lu, Y., LaCroix, L. B., Lowery, M. D., Solomon, E. I., Bender, C. J., Peisach, J., Roe, J. A., Gralla, E. B. & Valentine, J. S. (1993). *J. Am. Chem. Soc.* **115**, 5907–5918.

Murphy, L. M., Strange, R. W., Karlsson, G., Lundberg, L. G., Pascher, T., Reinhammar, B. & Hasnain, S. S. (1993). *Biochemistry*, **32**, 1965–1975.

Nar, H., Messerschmidt, A., Huber, R., van de Kamp, M. & Canters, G. W. (1991). *J. Mol. Biol.* **221**, 765–772.

Navaza, J. (1994). *Acta Cryst.* A**50**, 157–163.

Nishiyama, M., Suzuki, J., Kukimoto, M., Ohnuki, T., Horinouchi, S. & Beppu, T. (1993). *J. Gen. Microbiol.* **139**, 725–733.

Otwinowski, Z. (1993). *Proceedings of the CCP4 Study Weekend: Data Collection and Processing, 29–30 January*, compiled by L. Sawyer, N. Isaacs & S. Bailey, pp. 56–62. Warrington: Daresbury Laboratory.

Payne, W. (1985). In *Denitrification in the Nitrogen Cycle*, edited by H. L. Gloterman. New York: Plenum Press.

Romero, A., Hoitink, C. W. G., Nar, H., Huber, R., Messerschmidt, A. & Canters, G. W. (1991). *J. Mol. Biol.* **229**, 1007–1021.

Sakabe, N. (1991). *Nucl. Instrum. Methods A*, **303**, 448–463.

Scott, R. A., Hahn, J. E., Doniach, S., Freeman, H. C. & Hodgson, K. O. (1982). *J. Am. Chem. Soc.* **104**, 5364–5369

Strange, R. W., Dodd, F. E., Abraham, Z. H. L., Grossmann, J. G., Brüser, T., Eady, R. R., Smith, B. E. & Hasnain, S. S. (1995). *Nature Struct. Biol.* **2**, 287–292.

Strange, R. W., Murphy, L. M., Karlsson, G., Reinhammar, B. & Hasnain, S. S. (1996). *Biochemistry*, **35**, 16391–16398.

Thompson, A. W., Habash, J., Harrop, S., Helliwell, J. R., Nave, C., Atkinson, P., Hasnain, S. S., Glover, I. D., Moore, P., Haris, N., Kinder, S. & Buffy, S. (1992). *Rev. Sci. Instrum.* **63**, 1062–1065.

Ye, R. W., Averill, B. A. & Tiedje, J. M. (1992). *J. Bacteriol.* **174**, 6653–6658.

Wang, Y. N. & Averill, B. A. (1996). *J. Am. Chem. Soc.* **118**, 3972–3973

Weeg-Aerssens, E., Tiedje, J. M. & Averill, B. A. (1988). *J. Am. Chem. Soc.* **110**, 6851–6856.